Catalysis Today 269 (2016) 29–39

Catalysis Today

journal homepage: www.elsevier.com/locate/cattod

One-pot synthesis and recovery of fatty acid methyl esters (FAMEs) from microalgae biomass

Daniel R. Nelson [a], Sridhar Viamajala [b,*]

[a] Department of Biological Engineering, Utah State University, 4105 Old Main Hill, Logan, UT 84322-4105, United States
[b] Department of Chemical and Environmental Engineering, The University of Toledo, 3060 Nitschke Hall, MS 305, 2801 W. Bancroft St., Toledo, OH 43606-3390, United States

ARTICLE INFO

Article history:
Received 4 August 2015
Received in revised form
14 November 2015
Accepted 18 November 2015
Available online 15 February 2016

Keywords:
In situ transesterification
Algae
Biofuel
Biodiesel
Schizochytrium limacinum

ABSTRACT

We report a scalable method for recovery of cellular lipids and subsequent conversion to products. When in situ transesterification was performed at high solid loadings (>20%(w/w)) by reacting microalgal biomass in acidified methanol (containing 5%(v/v) H_2SO_4), the released FAMEs were produced at sufficiently high concentrations such that their solubility limit in the reaction medium was exceeded. As a result, the FAMEs *spontaneously* formed a separate phase lighter than methanol that could be directly recovered without solvent extraction. Further, FAME production rates were easily predicted, even in concentrated biomass slurries, by models derived from fundamental reaction kinetics. Our results also suggest that un-reacted methanol and catalyst, when recovered, could be reused in subsequent reactions. Thus, this "one-pot" process represents a viable method for production of biodiesel from algal biomass since this approach (1) eliminates costs associated with co-solvent (e.g., hexane) use, recovery and storage, (2) is easily scalable by virtue of the reaction not being constrained by mass transport limitations, and (3) facilitates processing of concentrated biomass slurries that would reduce reactor volumes and minimize reactor and handling costs.

1. Introduction

The environmental impacts of continued dependence on fossil fuels has created an urgent need for sustainable and renewable energy sources. It is estimated that fossil fuels consumed in one year generate 44×10^{15} kg of atmospheric carbon, which is 400-times the amount of annual carbon fixed by primary productivity of current global biota [19]. In the U.S., the amount of cellulosic ethanol from agricultural waste and other forest-based sources, which does not compete directly with food markets, could, at best, displace up to 30% of the national transportation fuel demand [48]. Additional lignocellulose-derived fuels could be generated from energy crops such as switch grass, but as recent studies show, changes in land use patterns to produce these crops could still result in a significant increase in carbon emissions [44]. In addition, the recently enacted Energy Independence and Security Act (EISA) of 2007 has set ambitious targets for "advanced biofuels" that must demonstrate at least 50% less greenhouse gas (GHG) emissions than petroleum-based alternatives. Clearly, fuels obtained from terrestrial lignocellulosic materials alone cannot sustainably bridge the impending energy gap or meet the renewable fuel mandates in the U.S. Alternative feedstocks such as microalgae that can be grown on non-arable lands, with low-quality water and without impacting existing agriculture and food markets, must be developed.

Biofuels produced from microalgae, at an estimated oil content of 40%, promise 10–100 times greater yield per land acre than other crops, are directly compatible with current combustion engines (drop-in fuels) and have the potential to significantly displace petroleum-based alternatives [1,7,9,14,16–18,45,52]. Microalgae are unicellular aquatic photosynthetic eukaryotes that fix CO_2 more efficiently than terrestrial plants [20,47]. Part of this fixed C is stored in various lipid forms, including triacylglycerides (TAGs), free fatty acids, sterols and wax esters – up to 60% of dry cell material in some strains [29,45]. Microalgae can also accumulate carbohydrate polymers (starchlike compounds) that could yield biofuels [15,17].

Lipids could be recovered from either wet or dry algal biomass. To extract lipids from wet algal pastes (after harvesting), methods based on the well-known Bligh and Dyer approach can be used [8]. In this procedure, a mixture of chloroform and methanol is added to wet biomass to perform the extraction and the sol-

* Corresponding author. Fax: +1 419 530 8086.
E-mail address: sridhar.viamajala@utoledo.edu (S. Viamajala).

http://dx.doi.org/10.1016/j.cattod.2015.11.048

vent ratios are balanced such that a single phase is formed with the sample water. After extraction is complete, phase separation is achieved by diluting the mixture with chloroform and water; and lipids partitioned into the organic phase can be recovered (for further conversion to fuel) by boiling off the chloroform. Most modifications or adaptations of this procedure involve changing the solvents and/or their ratios [13,21,34,41,53]. Besides requiring large volumes of solvent, extraction of wet biomass can produce significant solvent-contaminated wastewater that would require remediation. Furthermore, storage and handling of large volumes of volatile solvents poses safety hazards as well as environmental risks. In any case, lipid recovery from wet biomass is not very effective unless additional energy-intense cell disruption methods, such as sonication, high pressure homogenization, microwave or other thermochemical pretreatments, are applied in conjunction with solvent treatment [6,11,17,23,26]. Following extraction, a second step may be required—transesterification to make biodiesel or hydrotreatment to produce hydrocarbons. Thus, this overall two-step process requires significant amounts of solvents as well as multiple unit operations (including solvent recovery and storage). Although these methods can potentially be scaled-up to produce biodiesel from algae, the toxicity of the solvents and cost of their recovery are causes for concern.

Supercritical fluid extraction (SFE) using carbon dioxide [10,36] is an alternative approach that significantly lowers the requirements for organic solvents, as well as mitigates concerns for waste disposal after the reaction. SFE can also be performed on wet biomass using alcohols such as methanol [27] or ethanol [49]. In this process, solvent use is avoided and when used in combination with appropriate transesterification catalysts, methyl- or ethyl esters can be produced from biomass in a single step. However, this process requires high temperatures and pressures (250–350 °C and 50–200 atm pressure) [27,49], thus resulting in potentially high initial capital investment and continuously high energy inputs. Further, while laboratory scale studies show the potential of these methods for vegetable oils, their applicability to algal biomass is unknown. Finally, the scalability of these methods is yet to be established.

From dry biomass, lipids can be more easily extracted via solvent extraction [21,50] followed by evaporation of solvent. For conversion to biodiesel, these lipids have to be processed via transesterification with methanol. An alternative approach to recover lipids is via reactive extraction (or in-situ transesterification). In this method, extraction and transesterification are combined into a single step, thus lowering solvent use and processing time. For microalgae, acid catalysts are preferred in order to mitigate saponification and catalyst loss from free fatty acids present in the biomass [25]. Typically, substantially dry oleaginous biomass is treated with a mixture of alcohol and acid or base resulting in the reactive extraction of triglycerides as fatty acid alkyl esters (typically fatty acid methyl ester, or FAME). While dry biomass is preferred, recent studies have also shown that the method can give good yields in the presence of small amounts of moisture [40]. However, this process, as reported by others, results in a homogeneous methanol-FAME solution [2,12,30,34,38,42,51,54] and further liquid–liquid extraction (e.g., with chloroform or hexane) has to be applied to recover FAME from the reaction mixture.

In this report, we have outlined a simple and scalable strategy for reactive extraction of cellular lipids as FAMEs and their subsequent recovery as a distinct insoluble phase. We have further developed a first-principles kinetic model to predict the temporal formation of FAME product during in situ transesterification of microalgal biomass lipids as a function of biomass (or lipid) concentrations and catalyst loading.

2. Materials and methods

2.1. Chemicals

HPLC-grade chloroform, *n*-hexane, methanol were obtained from Sigma–Aldrich (St. Louis, MO) and used as received. Sulfuric acid (98%) and individual fatty acid methyl esters (all > 95% purity) including methyl myristate (C14:0), methyl pentadecanoate (C15:0), methyl palmitate (C 16:0), and methyl docosahexaenoate (C 22:6) were also obtained from Sigma–Aldrich and were used to prepare standards for gas chromatography (GC) calibrations. Yeast extract and Bacto-peptone were obtained from BD Biosciences (San Jose, CA). 99.5% pure glycerol was obtained from Mallinckrodt Chemicals (Phillipsburg, NJ). Instant Ocean brand sea salt was obtained from Aquarium Systems Inc. (Mentor, OH).

2.2. Microorganism, culture conditions and preparation of cells

A pure strain of *Schizochytrium limacinum* SR21 (ATCC MYA 1381, henceforth referred to as SR21) was used in this study. The growth medium contained 1 g/L yeast extract, 1 g/L peptone, 10 g/L sea salt, and 6 g/L glycerol that was adjusted to pH 7.0 and autoclaved. Cultures were grown in 5 L spinner flasks (Kontes Cytostir, Kimble Chase Life Science and Research Products LLC., Vineland, NJ) at room temperature (20 °C) and sparged with filtered air (0.2 μm). After 5 days, biomass from all growth reactors was harvested (4000 × *g*, 20 min), washed with a 0.85% (w/w) NaCl solution, and dehydrated using a FreeZone 4.5 freeze dryer (Labconco, Kansas City, MO).

2.3. In situ transesterification

The variables tested in this study included reaction temperature (60–100 °C), acid concentration (1–5% (v/v) H_2SO_4) and biomass concentration (66–250 mg/mL). The in-situ transesterification reactions were performed in 1.5 mL crimp-top GC vials. Freeze dried SR21 cells were first carefully weighed into dry vials followed by addition of 0.5–1 mL of acidified methanol solution. The acidified methanol solution was prepared by mixing appropriate volumes of concentrated sulfuric acid (98%) and methanol. The vials containing the mixture of biomass and acidified methanol were sealed and incubated in a heating block (model DRB200, Hach Chemical Company, Loveland, CO) for 10–180 min at set reaction temperature. The vials were removed every 10 min to be vortexed to ensure adequate mixing. Periodically, experimental vials were destructively sampled and analyzed for solubilized lipids and FAMEs. For each combination of temperature, acid-, and biomass-concentration, experiments incubated for various durations provided kinetic data for the reaction conditions.

For analysis, vials were removed from the heating block, cooled and centrifuged. The liquid was then carefully removed using a glass syringe and placed in a 20 mL serum bottle. 1 mL hexane was then added back into the reaction vials to rinse reactor contents of residual products. Vials were re-centrifuged and the supernatant was pooled with the original liquid product. 4 mL of hexane was further added to the serum bottles such that products of the in situ transesterification reaction were mixed with a total of 5 mL hexane. The serum bottles were sealed and extraction into hexane was performed by incubation at 90 °C for 20 min with vigorous shaking. After cooling, the acidified methanol and hexane formed separate phases. A 0.5 mL sample of the upper hexane phase was carefully removed, further diluted in hexane as required (to ensure measured

concentrations stayed within the calibration range) and placed in GC vials for analysis.

2.4. Extraction of native lipids

Native lipids were extracted from dry biomass using a solvent mixture containing equal volumes of hexane, tetrahydrofuran and chloroform similar to procedures previously reported [51]. 20 mg of freeze-dried biomass samples were sonicated (Model S-450A, Branson Ultrasonics Corporation, Dunbury, CT) in 5 mL of the solvent mixture at a power setting of approximately 150 W for 1 min in 10 s intervals. The tube was then centrifuged and the supernatant was collected. The extraction was repeated two more times by re-suspension of the pellet in fresh solvent followed by sonication. After each sonicaton step, the tube contents were centrifuged and all the supernatants were pooled together. Control tests showed that no measurable lipid was extractable beyond three repetitions of the extraction process. The pooled extract was filtered and analyzed by GC as described in Section 2.5.

2.5. Lipid analysis

A Shimadzu GC-2010 equipped with a Shimadzu AOC-20i auto injector and flame ionization detector (FID) was used for all analyses. The GC was equipped with a Restek RTX-Biodiesel column with 0.53 mm guard. The FID detector was set at 370 °C, with a column flow of 2.53 mL/min. The injection volume was 1 μL; temperature was programmed to increase from 60 °C to 370 °C at a rate of 10 °C/min and held constant at 370 °C for 6 min. FAME concentrations were calibrated over the range 0.025–0.3 mg/mL using standard solutions. Octocosane (0.1 mg/mL) was added to all standards and samples analyzed and served as an internal standard.

2.6. Statistical analysis

Each set of experiments was carried out in duplicate and all critical treatments were repeated as separate experiments to ensure reproducibility. Data presented here are the average values and error bars represent the computed standard deviation.

3. Results and discussion

3.1. Characterization of biomass lipids

Extraction was first performed on dry biomass using a solvent mixture (containing equal volumes of *n*-hexane, chloroform and tetrahydrofuran) that extracted lipids in their native state. The GC chromatograms of the "total lipid extract" showed that the majority of the cellular lipids were TAGs that eluted from the column at approximately 30–35 min [51]. Concentrations of other biodiesel-relevant components, such as mono- and di- glycerides or free fatty acids (elution times between 10–30 min) were comparatively much lower (Supplementary information Fig. S1). Consistent with previous analytical protocols, we also performed in situ transesterification with biomass at low concentrations in acidified methanol (20 mg/mL, 5%(v/v) H_2SO_4, 90 °C, 9 min) [25]. Extractions of reaction media and residues after in-situ transesterification did not show detectable TAGs suggesting that near-complete conversion to FAMEs was achieved. GC–MS analysis identified methyl palmitate and methyl docosohexanoate as the major FAME compounds along with smaller amounts of methyl myristate and methyl pentadecanoate eluting at 11 and 12 min, respectively. The fatty acid composition of SR21 obtained from FAME analysis is shown in Table 1 along with compositions reported by others [12,30,54].

3.2. Kinetic model development

As described by Meher et al. [37], the mechanism of transesterification catalyzed by Brønsted acids involves a three step process. In the first step, a carbonyl group of the glyceride is protonated to form a carbocation. This is followed by the nucleophilic attack of reacting alcohol (e.g., methanol) to produce a tetrahedral intermediate. This unstable intermediate finally gets eliminated from the glycerol backbone to form a new ester while simultaneously regenerating the proton catalyst. This general mechanism can be written in the form of the following three reaction steps:

$$G + H^+ \underset{k_{-1}}{\overset{k_1}{\rightleftharpoons}} GH^+ \quad (1)$$

$$GH^+ + M \underset{k_{-2}}{\overset{k_2}{\rightleftharpoons}} GMH^+ \quad (2)$$

$$GMH^+ \xrightarrow{k_3} FAME + Glycerol \quad (3)$$

where, G is the glyceride, M is methanol and H^+ is the proton. It must be noted that since this mechanism is written for one glyceride bond, the number of moles of FAME produced must equal the number of moles of glyceride bonds broken. Each triglyceride molecule has three glyceride bonds. The first two reactions are reversible with rate constants k_1, k_{-1}, k_2, and k_{-2} for the forward and reverse reactions. The third reaction is considered irreversible since the reaction is performed with large excess of methanol such that the molar glycerol concentrations would be very low. The rate constant for Reaction (3) is k_3.

From the three elementary reactions, the following equilibrium and rate relationships can be established:

$$k_1 [G] \left[H^+\right] = k_{-1} \left[GH^+\right] \quad (4)$$

$$k_2 \left[GH^+\right] [M] = k_{-2} \left[GMH^+\right] \quad (5)$$

$$k_3 \left[GMH^+\right] = \frac{d[FAME]}{dt} = -\frac{d[G]}{dt} \quad (6)$$

where,

[G] = specific stable glyceride concentration during the reaction (mM-glycride)

$\left[H^+\right]$ = specific stable H^+ concentration during the reaction (mM-H^+)

[M] = specific stable methanol concentration during the reaction (mM-methanol).

$\left[GH^+\right]$ = specific stable glyceride-H^+ carbocation during the reaction (mM-glyceride-H^+)

$\left[GMH^+\right]$ = specific stable glyceride-H^+-MeOH tetrahedral intermediate during the reaction (mM-glyceride-H^+-MeOH)

In this reaction, methanol is generally present in large stoichiometric excess and its concentration ([M]) can be assumed constant. The presence of excess methanol would also imply that the second reaction (Eq. (2)) rapidly attains equilibrium. The first reaction (Eq. (1)) is also assumed to be at equilibrium since it involves the relatively simple exchange of protons. Equilibrium relationships in Eqs. (4) and (5) can be used to establish the reciprocal equilibrium constants (k_a and k_b) for the first two steps of the reaction as:

$$k_a = \frac{k_{-1}}{k_1} = \frac{[G]\left[H^+\right]}{\left[GH^+\right]} \quad (7)$$

$$k_b = \frac{k_{-2}}{k_2} = \frac{\left[GH^+\right][M]}{\left[GMH^+\right]} \quad (8)$$

Table 1
Fatty acid methyl ester composition of *Schizochytrium limacinum* SR21.

References	Fatty acid composition (% w/w of total FAME)				FAME yield (% g-lipid/g-cell)
	Myristic (C14:0)	Pentadecanoic (C15:0)	Palmitic (C16:0)	DPA + DHA (C22:5 & C22:6)	
Yokochi et al. [54][a]	2.7	7.6	34.2	51.7	20
Chi et al. [12][a]	4.3	n.r.	52.5	42.8	44.7
Johnson and Wen [30][b]	5.3	n.r.	56.7	34.8	42.1
This study[a]	3.8 ± 0.1	2.5 ± 0.08	53.9 ± 1.3	40.1 ± 2.5	46.3 ± 1.2

n.r. = not reported.
DHA = docosahexaenoic acid; DPA = docosapentaenoic acid.
[a] Cultures grown on pure glycerol.
[b] Cultures grown on crude glycerol.

Using these identities, Eq. (6) can be rewritten as

$$k_3\left[GMH^+\right] = \frac{d[FAME]}{dt} = -\frac{d[G]}{dt} = k_3\frac{\left[GH^+\right][M]}{k_b}$$

$$= \frac{k_3[M]}{k_b} \times \frac{[G]\left[H^+\right]}{k_a} \quad (9)$$

In a simplified form,

$$\frac{d[FAME]}{dt} = -\frac{d[G]}{dt} = \frac{k_3}{k_a k_b}[G]\left[H^+\right][M] \quad (10)$$

Further, a mass balance of total proton concentration in the reactor can be written as:

$$\left[H^+\right]_0 = \left[H^+\right] + \left[GH^+\right] + \left[GMH^+\right] \quad (11)$$

where $\left[H^+\right]_0$ is the initial proton concentration at the start of the reaction and can be estimated from the amount of acid added to the reaction mixture.

$\left[GH^+\right]$ and $\left[\boldsymbol{G}MH^+\right]$ can be estimated from Eqs. (7) and (8) as

$$\left[GH^+\right] = \frac{[G]\left[H^+\right]}{k_a} \quad (12)$$

and,

$$\left[GMH^+\right] = \frac{\left[GH^+\right][M]}{k_b} = \frac{[G]\left[H^+\right][M]}{k_a k_b} \quad (13)$$

Substituting right hand side expressions from Eqs. (12) and (13) into Eq. (11) and rearranging terms, we get

$$\left[H^+\right] = \frac{\left[H^+\right]_0}{1 + \frac{[G]}{k_a} + \frac{[G][M]}{k_a k_b}} \quad (14)$$

Again, using the identity for $\left[H^+\right]$ from Eq. (14), Eq. (10) can be rearranged to give the expression for the overall rate equation as:

$$\frac{d[FAME]}{dt} = -\frac{d[G]}{dt} = \frac{k_3[M]\left[H^+\right]_0}{k_b\left(1 + \frac{[M]}{k_b}\right)} \times \frac{[G]}{\left(\frac{k_a}{1+\frac{[M]}{k_b}}\right) + [G]} \quad (15)$$

The first of the two product terms on the right hand side of Eq. (15) is nearly constant during an isothermal reaction performed at a set initial acid concentration ($\left[H^+\right]_0$) if [M] is in large stoichiometric excess and the equilibrium- and rate- constants remain unchanged. Thus, this term can be replaced by a single constant, V_m, as follows:

$$\frac{k_3 M\left[H^+\right]_0}{k_b\left(1 + \frac{[M]}{k_b}\right)} = V_m \quad (16)$$

In the second product term of Eq (15), while [G] changes during the reaction, the fractional term shown in parentheses in the in the denominator is also constant under isothermal reaction conditions and can be replaced by a single constant, K_m, as follows:

$$\frac{k_a}{1 + \frac{[M]}{k_b}} = K_m \quad (17)$$

Finally, the rate expression can be written in a simplified from similar to the Michaelis–Menten equation as:

$$\frac{d[FAME]}{dt} = -\frac{d[G]}{dt} = \frac{V_m[G]}{K_m + [G]} \quad (18)$$

While V_m and K_m would both change with temperature, V_m is also linearly proportional to the concentration of catalyst ($\left[H^+\right]_0$) used in the reaction. In the Michaelis–Menten model, V_m is similarly proportional to the initial enzyme concentration.

The equation can also be written in integrated form as

$$K_m \ln\left(\frac{[G]_0}{[G]}\right) + ([G]_0 - [G]) - V_m t = 0 \quad (19)$$

where $[G]_0$ is the initial glyceride concentration at the start of the reaction and t is any intermediate time point during the reaction. While the integrated form (Eq. (19)) is an exact solution to the differential Eq. (18), it remains an implicit non-linear equation. One simple approach to obtain an explicit closed-form solution to Eq. (18) is by using Lambert $W(x)$ functions [22]. Thus, an exact solution to Eq. (19) can be given as [43]

$$[G] = K_m \times W\left(\frac{[G]_0}{K_m}\exp\left(\frac{[G]_0 - V_m t}{K_m}\right)\right) \quad (20)$$

where the term in parentheses is the argument for the Lambert function. For any argument x, the a convenient, yet close, approximation of the Lambert function can be written as [4]

$$W(x) = (1+\varepsilon) \times \ln\left(\frac{6x}{5 \times \ln\left(\frac{2.4x}{\ln(1+2.4x)}\right)}\right) - \varepsilon \times \ln\left(\frac{2x}{\ln(1+2x)}\right) \quad (21)$$

where $\varepsilon = 0.4586887$

In terms of product concentrations, Eq. (20) becomes

$$[P] = [G]_0 - [G] = [G]_0 - K_m \times W\left(\frac{[G]_0}{K_m}\exp\left(\frac{[G]_0 - V_m t}{K_m}\right)\right) \quad (22)$$

The computations for Eqs. (21) and (22) can easily be realized on a computer spreadsheet (such as Excel) to generate [P] versus t data for systems with known kinetic parameters V_m and K_m. Alternately, given kinetic data, the constants can be estimated by using the Solver function in Microsoft Excel™, which uses a Generalized Reduced Gradient nonlinear optimization code, by providing initial guess values for the parameters and minimizing the error between sum of the squared differences between the observed and predicted [G] values.

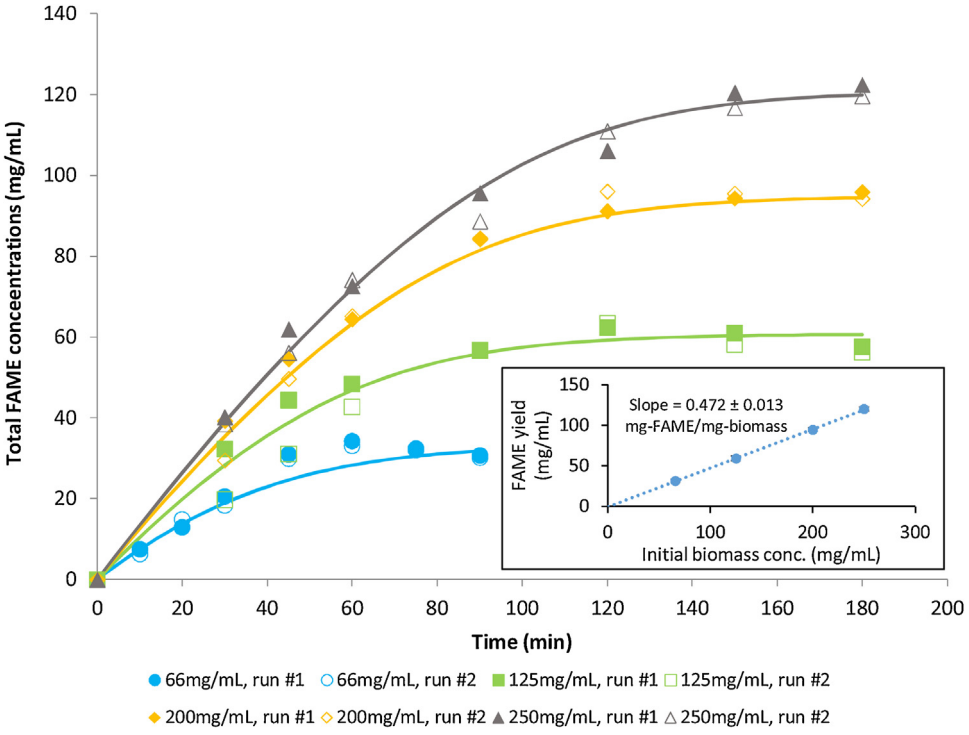

Fig. 1. Kinetics of in situ transesterification at varying initial biomass concentrations. The open and closed symbols in each color represent results from duplicate experimental runs. The solid lines represent model fits to experimental data. The color of the lines corresponds to the colors of the symbols that the model fit predicts. The inset to the graph shows FAME yield at the various initial biomass concentrations tested. The value of the slope of the linear regression line indicates the overall FAME yield across all the biomass concentrations tested.

3.3. Experimental kinetic data and model validation

Consistent with typical enzyme kinetic experiments, we first varied initial substrate (i.e., biomass) concentrations between 66 mg/mL and 250 mg/mL while keeping the catalyst loading constant (at 5%v/v; equal to an approximate sulfuric acid concentration of 95 mM). Reactions were performed isothermally at 90 °C and production of FAME was recorded over time. Experiments at each biomass concentration were performed in duplicate (marked run#1 and run#2 at each concentration). Methanol concentrations can be considered effectively unchanged during the reactions since even at the highest biomass loading (250 mg/mL), the molar ratio of methanol to triglyceride was approx. 60 while the stoichiometric ratio for transesterification is 3. From Fig. 1, it can be seen that the rates of reaction increased when higher substrate concentrations were used, as qualitatively predicted from Eq. (18). To quantitatively forecast the kinetics of FAME production, kinetic parameters from the explicit solution in Eq. (22) were estimated by global curve fitting for greater overall accuracy rather than obtaining kinetic constants for each progress curve. Although, Eq. (22) is written in terms of molar concentrations, the model equation will also be virtually identical in mass concentration units (mg/mL) since the molecular weights of the substrate (a single fatty acid chain attached to a glycerol backbone) and product (FAME) will be nearly equal. Model fits were therefore performed using product mass concentration data. $[G]_0$ was computed as the product of initial FAME content of the biomass (Table 1) and biomass concentrations used in the reaction. From this "global-fit multi progress-curve analysis", the kinetic constants were estimated to be:

$$V_m = 1.88\frac{\text{mg}}{\text{mL min}} \quad \text{and} \quad K_m = 44.76\frac{\text{mg}}{\text{mL}} \tag{23}$$

These kinetic constants were used to predict FAME production at all initial substrate concentrations. The results are shown as the solid lines in Fig. 1 and as can be seen, model fits were found to correspond very closely to experimental observations. The inset to Fig. 1 shows the average FAME yields at the various biomass concentrations tested in our experiments. From the slope of the regression line in the inset, the biomass yields are estimated to be 0.472 ± 0.013 mg-FAME/mg-biomass. These yields are consistent with our independent measurement of the FAME content of biomass as 0.463 ± 0.012 shown in Table 1.

To further assess if the model was broadly applicable, a second set of kinetic experiments were performed where biomass concentrations were kept constant (66 mg/mL), but catalyst (H_2SO_4) concentrations were varied (1–5% (v/v); approximately equal to molar concentrations of 19–95 mM). Reactions were performed isothermally at 90 °C. Under these conditions, K_m is expected to remain unchanged from the previously obtained estimate (Eq. (23)) due to identical reaction temperatures. However, V_m would change with initial catalyst concentration ($[H^+]_0$) (Eq. 16). As expected, the rates of FAME production increased when higher catalyst concentrations were applied (Fig. 2). The dashed line in Fig. 2 shows the theoretical FAME yield based on lipid composition reported in Table 1 and from the slope of the line shown in the inset to Fig. 1. A comparison with of theoretical yields with the experimental data shows two outliers (at 5% acid, $t = 60$ min) that have values which are significantly higher than expected, presumably due to experimental or measurement errors.

To estimate the kinetic parameters associated with reactions containing varying acid concentrations, independent curve fits were performed with duplicate time-course FAME production data that were experimentally obtained at each acid concentration. K_m from the previous estimate (44.76 mg/mL, Eq. (23)) was kept constant while V_m was allowed to vary to minimize errors between observed and predicted FAME concentrations. Thus, an independent V_m value was estimated at each acid concentration. Good correlation between experimental data (symbols) and model

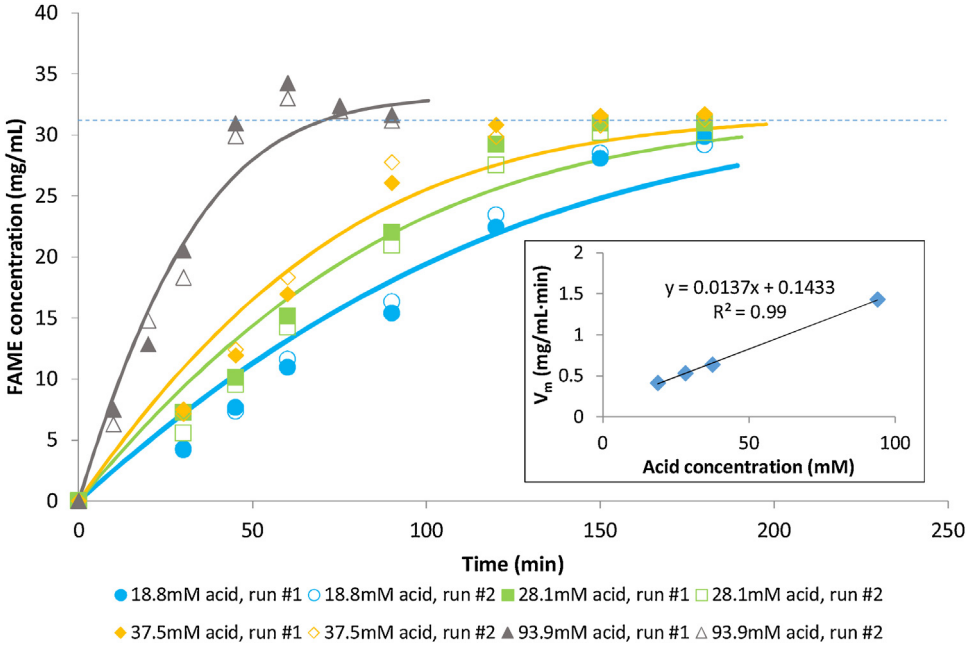

Fig. 2. Kinetics of in situ transesterification at varying acid (H_2SO_4) concentrations. The open and closed symbols in each color represent results from duplicate experimental runs. The solid lines represent model fits to experimental data. The color of the lines corresponds to the colors of the symbols that the model fit predicts. The horizontal dashed line indicates the theoretical FAME yield based on lipid content of the feed. The inset to the graph shows the linear correlation of the estimated kinetic parameter V_m with acid concentration. The equation of the regression line and the corresponding R^2 value of the regression fit are also shown in the inset.

predictions (lines) were also observed under these experimental conditions (Fig. 2).

Thereafter, to assess the correlation between model-generated V_m values and acid concentrations, we plotted V_m versus $\left[H^+\right]_0$ which is shown in the inset to Fig. 2. An exceptionally strong linear correlation was obtained, as expected from Eq. (16), further confirming the validity of the kinetic model. However, it is interesting to note that the linear regression line does not pass through the origin; rather the intercept is a small positive value which curiously suggests that biomass lipids would transesterify slowly even in the absence of a catalyst. It is possible that this low reactivity could be due to some of the Lewis acidic Al and Fe salts/minerals present in the solids (either as ash or from the growth medium) [35].

Finally, we assessed the effect of temperature on the reaction kinetics and these data are shown in Fig. 3. Experiments were performed at a biomass concentration of 66 mg/mL and with an acid concentration of 5% (v/v). The symbols represent average of duplicate experiments and error bars show one standard deviation from mean values. The solid lines in Fig. 3 do not represent model fits, but merely serve to connect the data points for visual clarity. As expected, rates (slopes of time–course curves) increased with increasing temperature with very slow reaction kinetics observed at 60 °C. Using zero-order initial rates (0–10 min), the effects of temperature on reaction kinetics were modeled using the Arrhenius equation (shown as inset to Fig. 3). Again, a good linear correlation was observed. For a multi-step reaction, as described here, involving multi-species equilibria, it is somewhat misleading to assess activation energies from the Arrhenius plot. However, the increase in rates with temperature do indicate that the progress of the third step of the reaction (Eq. (3)) is more rapid such that faster irreversible product generation occurs.

While several previous studies have assessed the impact of reaction variables such as acid concentration, time and reaction temperature on FAME production by in situ transesterification [25,28,30,40,51], a systematic and quantitative mechanism-based analysis of the reaction has not been reported. The framework presented here can potentially be applied to other experimental kinetic data available in the literature to assess the broad applicability of this model and determine species- and catalyst-specific variations in reaction kinetic parameters.

Although mathematical kinetic models for acid-catalyzed direct transesterification are absent in the literature, some efforts have been made to model base catalyzed transesterification reactions of triglycerides in vegetable oils [32,39]. However, base catalyzed transesterification occurs via a significantly different mechanism with mono- di- and triglycerides showing different degrees of reactivity. This results in accumulation of the intermediate glycerides *en route* to FAME formation. In the presence of excess methanol, base catalyzed transesterifications are believed to occur via a "shunt mechanism" where all glyceride bonds are simultaneously attacked. Since in situ transesterification also necessarily requires high methanol concentrations (to maintain a slurry of biomass during the reaction), it is possible that the variable reactivities of the glyceride bonds remain un-manifested. The model developed here implicitly assumes that all glyceride bonds have similar relativities and the close correlation of experimental data to model predictions shown here seems to support this hypothesis for in situ transesterification. Further, in GC chromatograms of samples taken during the course of the reactions, we did not detect the presence of mono-or di-glycerides.

One additional interesting implication of our results is that in situ transesterification appears to not be limited by mass transfer rates—our reaction vials were not continuously agitated and yet the reaction is well-described by from elementary mechanisms. When dry algal cells are suspended in methanol, the triglycerides present within the cells behave as a natural dispersion of oil in the polar reaction medium. The high lipid surface area available under these conditions likely drastically reduces mass transfer limitations and ensures rapid reaction.

3.4. Product recovery and recycle of unspent reaction media

During our studies, we made the unexpected observation that the FAMEs *spontaneously* formed a separate phase *lighter than*

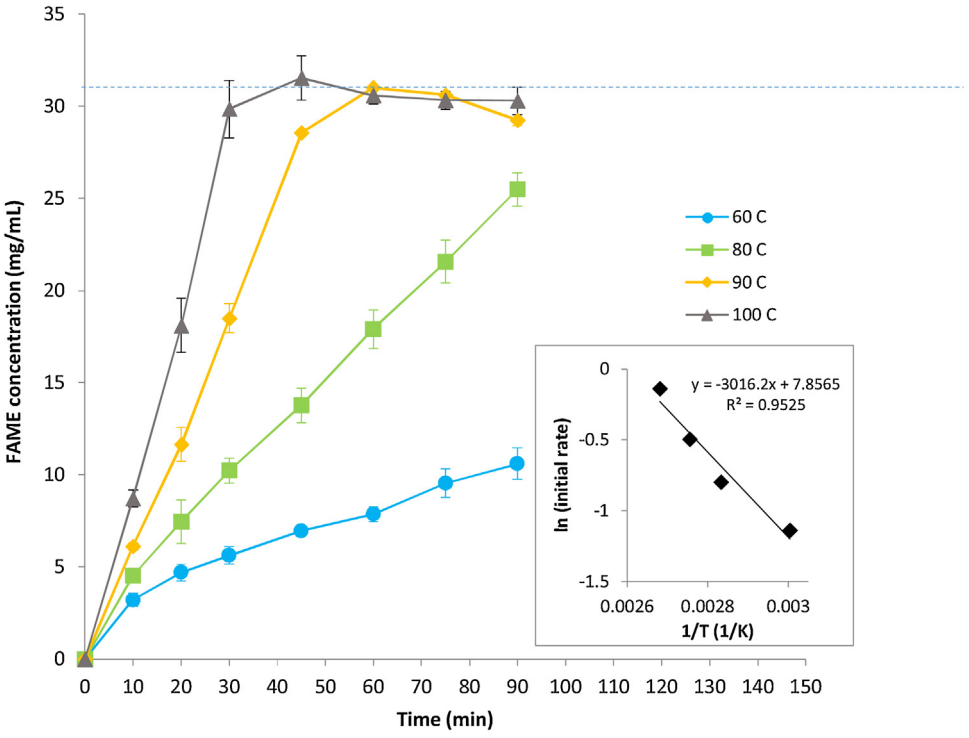

Fig. 3. Kinetics of in situ transesterification at varying reaction temperatures. Symbols represent experimental data points. The solid lines are connected to the data points for visual clarity of the data and do not represent model predictions. The horizontal dashed line indicates the theoretical FAME yield based on lipid content of the feed. The inset to the graph shows the Arrhenius correlation of initial rates to reaction temperature. The equation of the regression line and the corresponding R^2 value of the regression fit are also shown in the inset.

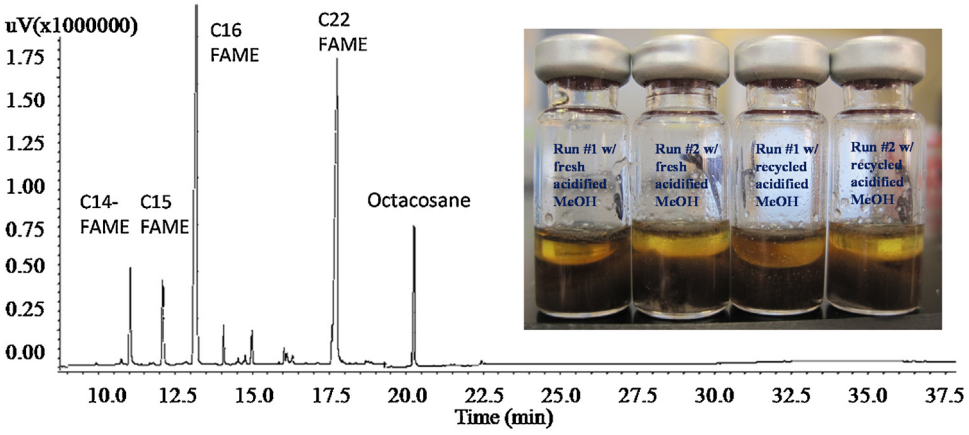

Fig. 4. GC chromatogram showing FAME products in the oil phase obtained after in situ transesterification reactions performed with a biomass concentration of 250 mg/mL at 90 °C with an H_2SO_4 catalyst concentration of 5% (v/v). The photograph shows the presence of a light FAME phase obtained after the reaction. The first two vials are duplicate experiments performed with fresh acidified methanol. The third and fourth vials are from duplicate experiments performed with recycled methanol.

methanol at the end of the reaction. The separate phase was most pronounced in reactions that contained high biomass (>20% (w/v)) and high acid (5% v/v) concentrations (see photograph in Fig. 4). The abundance of FAME in the light phase was evident when it was recovered and analyzed by GC (see chromatogram in Fig. 4). To assess the relative abundance of the product in the polar- and non-polar- phases, we independently measured the concentration of FAMEs in the entire reaction volume as well as in the methanol phase in reactions that contained varying initial substrate concentrations. Our results showed that the concentration of FAME in the methanol phase was approximately the same at all biomass loadings and approximately equal to 22 mg/mL (Fig. 5). The total FAME in the vial was much higher, especially in reactions with high substrate loadings. These results suggest that the polar phase has a low limited solubility for FAMEs such that phase separation spontaneously occurs when FAME concentrations exceed this solubility limit. In our experiments with the highest biomass concentrations tested (250 mg/mL), the product mixture is expected to comprise of 23.5 mmol-methanol (=0.95 mL), 0.4 mmol FAMEs (calculated using a biomass lipid content value of 46.3% and an average FAME molecular weight of 285 g/mole), and 0.13 mmol glycerol (assuming that 1 mol of glycerol is generated when 3 moles of FAME are produced). In this mixture, the mole fraction of methanol is >0.97. Previously reported phase equilibria [33,55] with the pure ternary methanol-glycerol-FAME mixtures suggest that a single miscible phase would form under these conditions; our results were contrary to this expectation. It was also somewhat puzzling, that the FAMEs formed a light phase, especially considering that the spe-

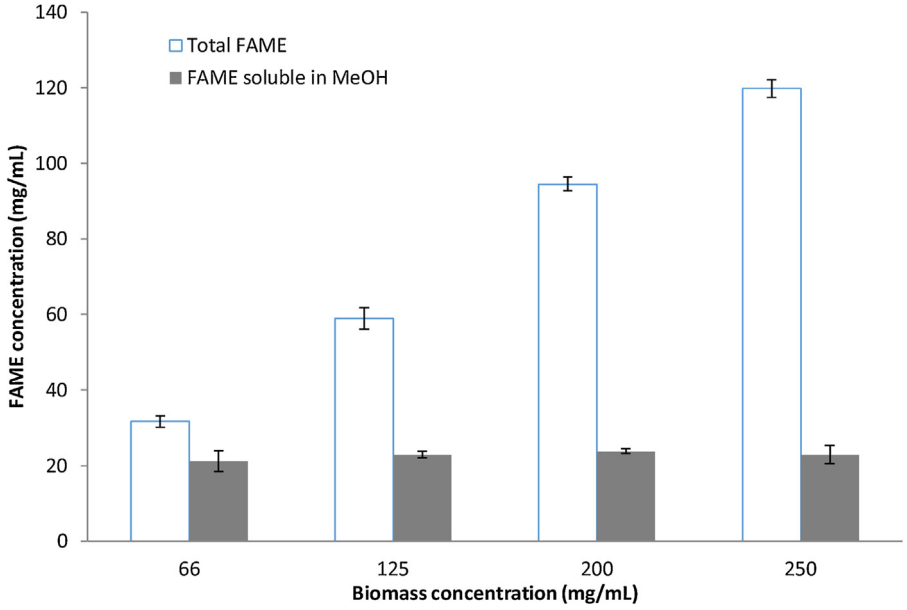

Fig. 5. Concentrations of soluble and insoluble FAMEs in the reaction vials after in situ transesterification performed at various biomass concentrations. Experiments were performed for 3 h at 90 °C with an H_2SO_4 catalyst concentration of 5% (v/v). The grey filled bars show the concentrations of FAME in the methanol phase and the empty bars show FAME concentration of the entire reaction mixture. FAME concentrations in the methanol phase were approximately 22 mg/mL at all biomass loadings.

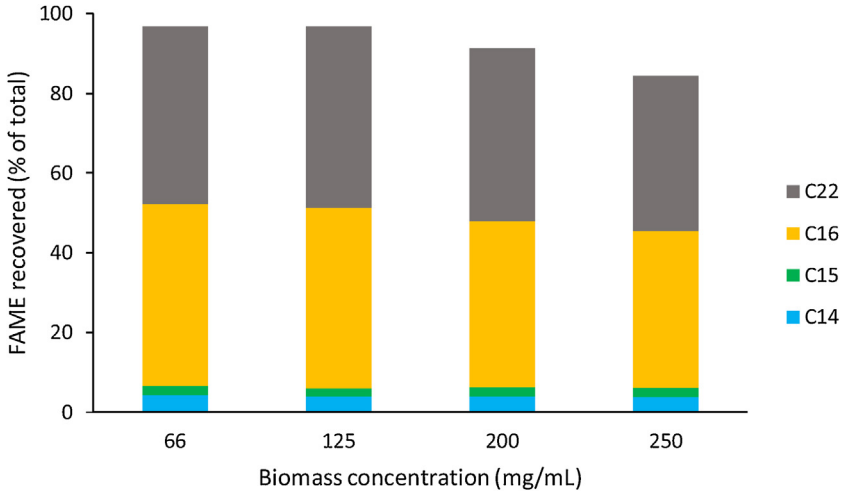

Fig. 6. FAME recoveries obtained from experiments performed at varying biomass loadings by utilizing recycled reaction media. Media from in situ transesterification reactions performed at a biomass loading of 200 mg/mL and containing 5% (v/v) acid were recovered and used in these experiments. Reaction yields varied between 95% (low biomass loadings) and 85% (high biomass loadings).

cific gravity of FAMEs is higher than methanol – sp. gr. of methanol 0.79 and that of most FAMEs is approximately 0.85–0.87. However, H_2SO_4 has a high specific gravity (1.84) which would cause an increase in the overall density of the reaction medium. An acidified methanol solution containing 0.05 mL H_2SO_4 and 0.95 mL methanol is expected to have a density of approximately 0.84 g/mL (calculated using an H_2SO_4 sp. gr. of 1.84). Further, algal biomass contains associated media salts and ash, which if solubilized in the polar methanol would also increase the reaction medium density and perhaps also facilitate good phase separation by increasing the interfacial surface tension. For example, for a feed with ash content of 10% (w/w) (typical of microalgae), the amount of minerals present in the medium, for a reaction with 250 mg biomass, would be approximately 25 mg. When solubilized in methanol, this would further significantly increase the density of the methanol phase (up to 0.865 mg/mL). The more miscible acid and salt solutes could also possibly lower the effective solubility of FAME in methanol. Additionally, the in situ transesterification process would also likely solubilize cellular materials which would further increase the density of the methanol phase. If 50 mg (out of the 250 mg feed) were solubilized during the reaction (due to release of cellular material as a result of cell lysis during reaction or formation of glycosides from carbohydrates), the density of the methanol phase could conceivably exceed the density of FAMEs. One final possibility is that the density of the FAME phase could have decreased due to dissolution of methanol in that phase. It has been previously estimated that the methanol content of biodiesel after transesterification of vegetable oils is typically 2–4% [31]. At this low solubility, the density of the FAME phase would be decreased (from 0.87 g/mL to 0.867 g/mL), but not substantially. In any case, without accurate measurements of the various non-FAME components (organic and inorganic) in the methanol phase, it is difficult to accurately assess which factors contributed to the formation of a dense phase. Our ongoing studies are further investigating this unexpected phase behavior.

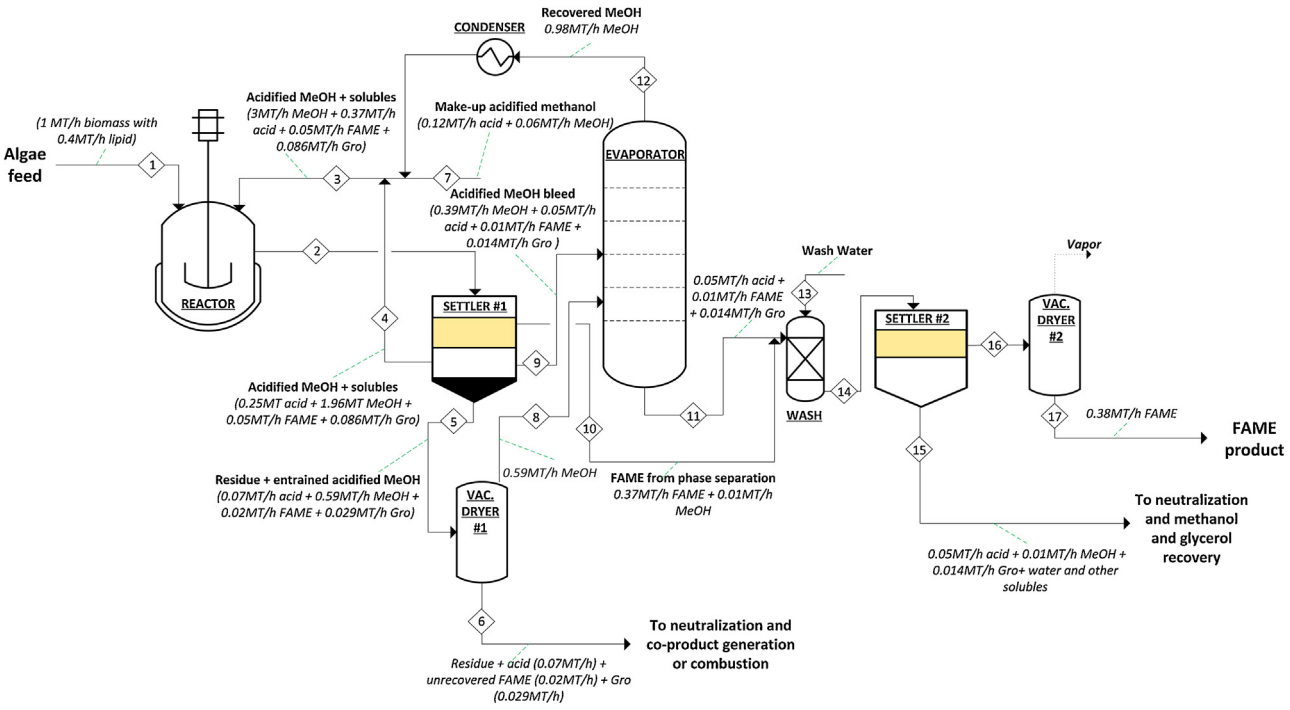

Fig. 7. Conceptual design of a process that employs in situ transesterification followed by FAME recovery as a separate phase. Mass balances (stream data) are shown for an algae biomass feed rate of 1MT/h and 40% (w/w) lipid content. Mass balance calculations are based on experimentally obtained data during this study. The green dashed lines point to stream mass flow data. Glycerol is abbreviated as Gro.

Next, to assess the reusability of the reaction media, we recovered the polar phase (comprising of remaining methanol, acid, soluble FAMEs and other by-products of the reaction) and used it (without any modification) to perform a second in situ transesterification. The polar liquid phase was carefully recovered from reaction vials that had been used to complete a first transesterification reaction (reacted at 90 °C) with 20% (w/v) solids in acidified methanol containing 5% (v/v) H_2SO_4. The second set of reactions were carried out at four biomass concentrations—66, 125, 200 and 250 mg/mL. Lipid yield was determined after appropriately accounting for soluble lipids from the previous transesterification step and the results of FAME recovery with the recycled reactant are shown in Fig. 6. These data show that nearly 100% recovery of lipids was obtained when low biomass concentrations were used. At high biomass concentrations, at least 85% of the lipids were transformed into FAMEs during the 3 h reaction period. It is possible that sufficient accumulation of glycerol occurs during the two-reaction sequence such that the forward methyl ester formation reaction in inhibited. It is also possible that some acid was consumed due to neutralization of basic amino acids during the course of the two sequential reactions and may have lowered the effective catalyst concentration resulting in lower reaction rates (Fig. 2). A simple "bleed" strategy of replacing a portion or the spent reaction media with fresh acidified methanol prior to the second step, could possibly lower the effective glycerol concentrations as well as replenish spent catalyst and continue to deliver stoichiometric yields. From our results, it appears that quantitative conversions at high solids concentrations (25% (w/w)) could be achieved with a bleed of 20% of the reaction media.

The formation of FAME as a separate phase and the potential for substantial reuse of the reaction media would have significant impact on the overall processing costs as well as on the environmental sustainability of lipid-derived fuels from algae. First, recovery of FAME by phase separation would avoid the use of extraction solvents for FAME recovery. As recently described, a solvent to biomass feed ratio of 5:1 is expected to be needed for extraction of lipids from slurries in a multi-stage process [17]—nearly equal to the amount of methanol used if reacting concentrated biomass slurries with 20% solids. If hexane is used for extraction, the energy burden associate with solvent recovery would be nearly 2 MJ per kg biomass processed (based on evaporation of hexane, enthalpy of vaporization = 0.365 MJ/kg). The process would further incur other costs associated with purchase of extraction equipment and energy for mixing. In addition, storage and handling of large volumes of volatile, toxic and flammable solvents poses serious safety and environmental risks. Re-use of the reaction media also lowers the burden associated with purchase of fresh catalyst and methanol evaporation. If 80% of the reaction media could be recycled directly, methanol recovery costs (from distillation) would also be significantly lowered.

3.5. Conceptual process flow diagram

Based on our experimental results, we have developed a conceptual design of a process for direct transesterification and FAME production (Fig. 7). Mass balances are shown for a process feed of 1 MT/h biomass with a lipid content of 40% (w/w). After reaction with (recycled) acidified methanol (stream 3), the product (stream 2) is sent to Settler #1 for phase separation and recovery of FAME. During transesterification, 0.05 MT/h of methanol is consumed and 0.043 MT/h of glycerol is produced. In addition, a small portion of methanol is solubilized into the FAME phase. From the literature, the FAME phase contains 2–4% methanol [31]. Using an average value of 3%, the methanol mass flow in the FAME phase is approximately 0.01 MT/h. Glycerol is considered to be insoluble in the FAME [31]. The majority of FAME product is directly recovered from Settler #1 (stream 10) and sent for downstream product purification. Two-thirds of the remaining acidified methanol (after losses to transesterification and dissolution in FAME) from Settler #1 is directly recycled back to the reactor (stream 4). This phase also contains FAME at a concentration of 22 mg/mL based on its solubility in acidified methanol as estimated in the previous section. A

part of the acidified methanol leaves from the bottom of the settler due to entrainment with the solids (stream 5). The "bleed" stream 9 removes the remainder of the acidified methanol from the settler. Glycerol is removed from the system with streams 5 and 9 and the new mass of glycerol produced must equal the mass of glycerol leaving the recycle loop. From mass balances (assuming two-thirds flow to stream 5 and one-third flow to stream 9), glycerol flow rate in streams 5 and 9 will be 0.029 MT/h and 0.014 MT/h, respectively. Further, since flow of stream 4 is two-fold higher than the sum of the flows in the bleed streams (stream 5 and 9), the flow rate of glycerol in stream 4 will be 0.086 MT/h. The wet residues from Settler #1 are sent to a dryer for methanol recovery. The hot methanol vapors from the dryer are sent to an evaporator which also receives the bleed stream. The hot and cold methanol streams (streams 8 and 9) are combined in the evaporator for energy integration. The bottoms product of Vacuum dryer #1 (stream 6) contains post-extraction residues and along with small amounts of non-volatile acid, FAME and glycerol which could be further processed for nutrient/glycerol recovery or co-product generation from the residue. Methanol vapors from the evaporator (stream 12) are condensed and recycled back to the reactor. Fresh make-up acid and methanol are also fed to the reactor (stream 7) to compensate for losses in streams 6 and 11 and methanol consumption during transesterification. FAME from Settler #1 and evaporator bottoms (stream 11) is combined and sent to a water wash to remove acid, glycerol, methanol and other solubles similar to the conventional practice in the biodiesel industry [24]. The "washed" FAME is recovered by settling (Settler #2) and dehydrated in Dryer #2 to finally obtain a usable fuel product. The wash water from Settler #2 is sent for methanol and glycerol recovery.

From this process flow, methanol could be used in a closed loop with significant portions being directly recycled without evaporation. While the feasibility of this approach of prolonged recycle of the reaction media has not been rigorously proven in the present study, our results certainly point to the feasibility of partial reaction media reuse. Use of fresh sulfuric acid would also be significantly lower due to recycle. The primary energy burden for this process would come from evaporation of methanol. From our mass balance, 1 MT/h of methanol would be evaporated with an energy demand of 1.1 GJ/h (based on enthalpy of vaporization of methanol). Assuming stoichiometric yields in the reactor (as evidenced from our kinetic experiments) 95% of the incoming lipids could be recovered without use of solvents.

Although not directly addressed in this study, biomass (feed) drying costs need to be considered in the overall energy calculations of the process. Since estimates of moisture content after harvesting and dewatering vary widely based on different technologies that are available (typically between 70–90% (w/w) depending upon use of centrifuge and/or belt press) [3], evaluation of these upstream processes is outside the scope of the work being presented here. However, at some geographical locations of the world (such as tropical regions), fossil energy needs for drying may be lowered through use of cross-flow air drying or solar drying [5,46].

4. Conclusions

In this study, we have developed a comprehensive understanding of the direct transesterification reaction for recovering FAMEs from microalgae. We have demonstrated that the process can be simplified and the energy efficiency can be improved through processing concentrated biomass slurries. In addition to reducing reactor volumes, this high solids processing approach allows the recovery of FAMEs through automatic phase separation without solvent extraction. The accurate prediction of reaction progress by the kinetic model developed here suggests that direct transesterification is unlikely to be mass transfer limited. This would facilitate scalable reactor designs and predictable operation. The kinetic model developed herein can be used for developing scalable reactor designs. Finally, our process wide mass balances suggest a high degree of recyclability of unspent reactants and catalyst.

Acknowledgements

This project was supported by (1) the National Science Foundation through the Sustainable Energy Pathways Program (award# CHE-1230609), (2) the US Department of Energy Bioenergy Technologies Office (award# DE-EE0005993) and (3) the Utah Science Technology and Research Initiative (USTAR).

Appendix A. Supplementary data

Supplementary data associated with this article can be found, in the online version, at http://dx.doi.org/10.1016/j.cattod.2015.11.048.

References

[1] S. Aaronson, T. Berner, Z. Dubinsky, Microalgae as a source of chemicals and natural products, in: G. Shelef, C.J. Soeder (Eds.), Algae Biomass, Production and Use, Elsevier/North-Holland Biomedical Press, Amsterdam, 1980, pp. 575–601.
[2] A. Ashford, W.R. Barclay, C.A. Weaver, T.H. Giddings, S. Zeller, Electron microscopy may reveal structure of docosahexaenoic acid-rich oil within *Schizochytrium* sp, Lipids 35 (2000) 1377–1386.
[3] A.I. Barros, A.L. Gonçalves, M. Simões, J.C.M. Pires, Harvesting techniques applied to microalgae: a review, Renewable Sustainable Energy Rev. 41 (2015) 1489–1500.
[4] D.A. Barry, J.Y. Parlange, L. Li, H. Prommer, C.J. Cunningham, F. Stagnitti, Analytical approximations for real values of the Lambert W-function, Math. Comput. Simul. 53 (2000) 95–103.
[5] E.W. Becker, L.V. Venkataraman, Biotechnology and Exploitation of Algae: The Indian Approach: A Comprehensive Report on the Cultivation and Utilization of Microalgae Performed at the Central Food Technological Research Institute, German Agency for Technical Cooperation, Mysore, India, 1982.
[6] E.H. Belarbi, E. Molina, Y. Chisti, A process for high yield and scaleable recovery of high purity eicosapentaenoic acid esters from microalgae and fish oil, Enzyme Microb. Technol. 26 (2000) 516–529.
[7] J. Benemann, CO_2 mitigation with microalgae systems, Energy Convers. Manage. 38 (1997) 475–480.
[8] E.G. Bligh, W.J. Dyer, A rapid method for total lipid extraction and purification, Can. J. Biochem. Physiol. 37 (1959) 911–917.
[9] M.A. Borowitzka, Commercial Production of Microalgae: Ponds, Tanks, Tubes and Fermenters, Elsevier Science B.V., 1999, pp. 313–321.
[10] A.I. Carrapiso, C. Garcia, Development in lipid analysis: some new extraction techniques and in situ transesterification, Lipids 35 (2000) 1167–1177.
[11] J. Cheng, T. Yu, T. Li, J. Zhou, K. Cen, Using wet microalgae for direct biodiesel production via microwave irradiation, Bioresour. Technol. 131 (2013) 531–535.
[12] Z.Y. Chi, D. Pyle, Z.Y. Wen, C. Frear, S.L. Chen, A laboratory study of producing docosahexaenoic acid from biodiesel-waste glycerol by microalgal fermentation, Process Biochem. 42 (2007) 1537–1545.
[13] H.J. Chin, T.F. Shen, H.P. Su, S.T. Ding, *Schizochytrium limacinum* SR-21 as a source of docosahexaenoic acid: optimal growth and use as a dietary supplement for laying hens, Aust. J. Agric. Res. 57 (2006) 13–20.
[14] Y. Chisti, Biodiesel from microalgae, Biotechnol. Adv. 25 (2007) 294–306.
[15] J. Courtois, Oligosaccharides from land plants and algae: production and applications in therapeutics and biotechnology, Curr. Opin. Microbiol. 12 (2009) 261–273.
[16] R. Davis, D. Fishman, E.D. Frank, M.S. Wigmosta, A. Aden, A.M. Coleman, P.T. Pienkos, R.J. Skaggs, E.R. Venteris, M.Q. Wang, Renewable Diesel from Algal Lipids: An Integrated Baseline for Cos. Emissions and Resource Potential from a Harmonized Model, 2012 pp. Medium: ED; Size: 85 pp.
[17] R. Davis, C. Kinchin, J. Markham, E. Tan, L. Laurens, D. Sexton, D. Knorr, P. Schoen, J. Lukas, Process Design and Economics for the Conversion of Algal Biomass to Biofuels: Algal Biomass Fractionation to Lipid- and Carbohydrate-Derived Fuel Products 2014, pp. Medium: ED; Size: 110 pp.
[18] U.S. DOE, National Algal Biofuels Technology Roadmap, U.S Department of Energy Office of Energy Efficiency and Renewable Energy, Biomass Program, (2010).
[19] J.S. Dukes, Burning buried sunshine: human consumption of ancient solar energy, Clim. Change 61 (2003) 31–44.
[20] G. Fogg, B. Thake, Algal Cultures and Phytoplankton Ecology, University of Wisconsin Press, 1987.

[21] J. Folch, M. Lees, G.H.S. Stanley, A simple method for the isolation and purification of total lipids from animal tissues, J. Biol. Chem. 226 (1957) 497–509.
[22] M. Goličnik, Exact and approximate solutions for the decades-old Michaelis–Menten equation: progress-curve analysis through integrated rate equations, Biochem. Mol. Biol. Educ. 39 (2011) 117–125.
[23] A. Guldhe, B. Singh, I. Rawat, K. Ramluckan, F. Bux, Efficacy of drying and cell disruption techniques on lipid recovery from microalgae for biodiesel production, Fuel 128 (2014) 46–52.
[24] M.J. Haas, A.J. McAloon, W.C. Yee, T.A. Foglia, A process model to estimate biodiesel production costs, Bioresour. Technol. 97 (2006) 671–678.
[25] M.J. Haas, K. Wagner, Simplifying biodiesel production: the direct or in situ transesterification of algal biomass, Eur. J. Lipid Sci. Technol. 113 (2011) 1219–1229.
[26] R. Halim, R. Harun, M.K. Danquah, P.A. Webley, Microalgal cell disruption for biofuel development, Appl. Energy 91 (2012) 116–121.
[27] S. Hawash, N. Kamal, F. Zaher, O. Kenawi, G.E. Diwani, Biodiesel fuel from Jatropha oil via non-catalytic supercritical methanol transesterification, Fuel 88 (2009) 579–582.
[28] P. Hidalgo, C. Toro, G. Ciudad, R. Navia, Advances in direct transesterification of microalgal biomass for biodiesel production, Rev. Environ. Sci. Biotechnol. 12 (2013) 179–199.
[29] Q. Hu, M. Sommerfeld, E. Jarvis, M. Ghirardi, M. Posewitz, M. Seibert, A. Darzins, Microalgal triacylglycerols as feedstocks for biofuel production: perspectives and advances, Plant J. 54 (2008) 621–639.
[30] M.B. Johnson, Z. Wen, Production of biodiesel fuel from the microalga *Schizochytrium limacinum* by direct transesterification of algal biomass, Energy Fuels 23 (2009) 5179–5183.
[31] G. Knothe, J. Krahl, J. Van Gerpen, The Biodiesel Handbook, Elsevier Science, 2015.
[32] K. Komers, F. Skopal, R. Stloukal, J. Machek, Kinetics and mechanism of the KOH—catalyzed methanolysis of rapeseed oil for biodiesel production, Eur. J. Lipid Sci. Technol. 104 (2002) 728–737.
[33] M.-J. Lee, Y.-C. Lo, H.-M. Lin, Liquid–liquid equilibria for mixtures containing water, methanol, fatty acid methyl esters, and glycerol, Fluid Phase Equilib. 299 (2010) 180–190.
[34] T. Lewis, P.D. Nichols, T.A. McMeekin, Evaluation of extraction methods for recovery of fatty acids from lipid-producing microheterotrophs, J. Microbiol. Methods 43 (2000) 107–116.
[35] E. Lotero, Y. Liu, D.E. Lopez, K. Suwannakarn, D.A. Bruce, J.G. Goodwin, Synthesis of biodiesel via acid catalysis, Ind. Eng. Chem. Res. 44 (2005) 5353–5363.
[36] J.M. Marchetti, V.U. Miguel, A.F. Errazu, Possible methods for biodiesel production, Renewable Sustainable Energy Rev. 11 (2007) 1300–1311.
[37] L.C. Meher, D. Vidya Sagar, S.N. Naik, Technical aspects of biodiesel production by transesterification—a review, Renewable Sustainable Energy Rev. 10 (2006) 248–268.
[38] E. Morita, Y. Kumon, T. Nakahara, S. Kagiwada, T. Noguchi, Docosahexaenoic acid production and lipid-body formation in *Schizochytrium limacinum* SR21, Mar. Biotechnol. 8 (2006) 319–327.
[39] H. Noureddini, D. Zhu, Kinetics of transesterification of soybean oil, J. Am. Oil Chem. Soc. 74 (1997) 1457–1463.
[40] J.-Y. Park, M.S. Park, Y.-C. Lee, J.-W. Yang, Advances in direct transesterification of algal oils from wet biomass, Bioresour. Technol. 184 (2015) 267–275.
[41] Z. Perveen, H. Ando, A. Ueno, Y. Ito, Y. Yamamoto, Y. Yamada, T. Takagi, T. Kaneko, K. Kogame, H. Okuyama, Isolation and characterization of a novel thraustochytrid-like microorganism that efficiently produces docosahexaenoic acid, Biotechnol. Lett. 28 (2006) 197–202.
[42] E. Revellame, R. Hernandez, W. French, W. Holmes, E. Alley, Biodiesel from activated sludge through in situ transesterification, J. Chem. Technol. Biotechnol. 85 (2010) 614–620.
[43] S. Schnell, C. Mendoza, Closed form solution for time-dependent enzyme kinetics, J. Theor. Biol. 187 (1997) 207–212.
[44] T. Searchinger, R. Heimlich, R.A. Houghton, F. Dong, A. Elobeid, J. Fabiosa, S. Tokgoz, D. Hayes, T.H. Yu, Use of US croplands for biofuels increases greenhouse gases through emissions from land-use change, Science 319 (2008) 1238.
[45] J. Sheehan, T. Dunahay, J.R. Benemann, P. Roessler, A Look Back at the U.S. Department of Energy's Aquatic Species Program—Biodiesel from Algae, National Renewable Energy Laboratory, Golden, Colorado, 1998.
[46] K.-Y. Show, D.-J. Lee, J.-H. Tay, T.-M. Lee, J.-S. Chang, Microalgal drying and cell disruption—recent advances, Bioresour. Technol. 184 (2015) 258–266.
[47] A. Sukenik, P.G. Falkowski, J. Bennett, Potential enhancement of photosynthetic energy-conversion in algal mass culture, Biotechnol. Bioeng. 30 (1987) 970–977.
[48] USDOE, Multi-Year Program Plan, 2007–2012, Office of the Biomass Program, Washington DC, 2005, http://www1.eere.energy.gov/biomass/pdfs/mypp.pdf.
[49] I. Vieitez, C. da Silva, I. Alckmin, G.R. Borges, F.C. Corazza, J.V. Oliveira, M.A. Grompone, I. Jachmanián, Effect of temperature on the continuous synthesis of soybean esters under supercritical ethanol, Energy Fuels 23 (2008) 558–563.
[50] B.D. Wahlen, B.M. Barney, L.C. Seefeldt, Synthesis of biodiesel from mixed feedstocks and longer chain alcohols using an acid-catalyzed method, Energy Fuels 22 (2008) 4223–4228.
[51] B.D. Wahlen, R.M. Willis, L.C. Seefeldt, Biodiesel production by simultaneous extraction and conversion of total lipids from microalgae, cyanobacteria, and wild mixed-cultures, Bioresour. Technol. 102 (2010) 2724–2730.
[52] R.H. Wijffels, M.J. Barbosa, An outlook on microalgal biofuels, Science 329 (2010) 796–799.
[53] S.T. Wu, S.T. Yu, L.P. Lin, Effect of culture conditions on docosahexaenoic acid production by Schizochytrium sp S31, Process Biochem. 40 (2005) 3103–3108.
[54] T. Yokochi, D. Honda, T. Higashihara, T. Nakahara, Optimization of docosahexaenoic acid production by *Schizochytrium limacinum* SR21, Appl. Microbiol. Biotechnol. 49 (1998) 72–76.
[55] H. Zhou, H. Lu, B. Liang, Solubility of multicomponent systems in the biodiesel production by transesterification of *Jatropha curcas* L. oil with methanol, J. Chem. Eng. Data 51 (2006) 1130–1135.